Reconstruction and identification of $H \to WW^*$ with high transverse momentum in the full hadronic final state

Chunhui Chen

Department of Physics and Astronomy, Iowa State University, Ames, Iowa 50011, USA

(Received 4 December 2020; accepted 8 February 2021; published 24 February 2021)

This paper presents a study of the reconstruction and identification of $H \to WW^*$ with high transverse momentum, where both $W^{(*)}$ bosons decay hadronically. We show that the boosted $H \to WW^*$ can be effectively reconstructed as a single jet and identified using jet substructures in the center-of-mass frame of the jet. Such a reconstruction and identification approach can discriminate the boosted $H \to WW^*$ in the full hadronic final state from QCD jets. This result will significantly improve experimental sensitivities of searches for potential new physics phenomena beyond the standard model in final states containing highly boosted Higgs bosons.

DOI: 10.1103/PhysRevD.103.033005

I. INTRODUCTION

Many new physics (NP) extensions to the standard model (SM) predict new particles with masses at the TeV scale. Some of these heavy resonances [1–5] can decay into final states containing Higgs bosons. The most effective way to search for such particles is to reconstruct the Higgs boson in its dominant decay into a bottom quark-antiquark pair ($b\bar{b}$) final state. Because the Higgs bosons decayed from heavy resonances have very large momenta (boosted), the hadronically decaying products of $H \to b\bar{b}$ are so collimated that they are often reconstructed as single jets in the experiments. The search for new heavy resonances using the signature of boosted $H \to b\bar{b}$ is an emerging field of research that has attracted significant theoretical and experimental interests [6–8]. While the current searches by both the ATLAS [9–23] and CMS [24–36] experiments at the Large Hadron Collider (LHC) start to probe heavy resonances with masses as large as 2–3 TeV, the experimental sensitivities become limited by the signal reconstruction efficiency as the production cross sections of both heavy resonances and background from the SM processes drop significantly at the very high energy scale.

In this paper, we present a study of the reconstruction and identification of boosted $H \to WW^*$, where both the on-shell W boson and the off-shell W^* boson decay hadronically. The $H \to WW^*$ decay mode has the second-largest decaying branch fraction of 21%, and there have not been any published studies on its boosted signature. We show that a boosted $H \to WW^*$ in the hadronic final state can be effectively reconstructed as a single jet, hereafter referred to as a $H \to WW^*$ jet. By using jet substructures in the center-of-mass frame of the jet, the $H \to WW^*$ jets can be distinguished from QCD jets, where the QCD jets are defined as those jets initiated by a nontop quark or a gluon. This result can significantly improve experimental sensitivities of searches for potential NP phenomena in final states containing highly boosted Higgs bosons.

II. EVENT SAMPLE

We use the boosted $H \to WW^*$ jets, from the SM process of ZH production, as a benchmark to study the signal reconstruction and identification. The SM multijet production process is used to model the QCD jets. The sample of $H \to WW^*$ jets is further reweighted on a jet-by-jet basis such that its jet kinematics in transverse momentum (p_T) and pseudorapidity (η) match that of the QCD jet sample.

All the events used in this analysis are produced using the PYTHIA8.244 Monte Carlo (MC) event generator [37,38] for the pp collision at 13 TeV center-of-mass energy. The spread of beam interaction point is assumed to follow a Gaussian distribution with a width of 0.015 mm in the transverse beam direction and 45 mm in the longitudinal beam direction [39]. We divide the (η, ϕ) plane into 0.1×0.1 cells to simulate the finite resolution of the calorimeter detector at the LHC experiments. The energies of particles entering each cell in each event, except for the neutrinos, are summed over and replaced with a massless pseudoparticle of the same energy, also referred to as an energy cluster, pointing to the center of the cell.

These pseudoparticles are fed into the FASTJET3.0.1 [40] package for jet reconstruction. As for charged tracks, their momenta and vertex positions are smeared according to the expected resolutions of the ATLAS detector [41]. The effect of multiple pp interactions in the same event (pileup) is included by overlaying minimum-bias events simulated with PYTHIA8.244 on each event of interest in all samples. The number of pileup events is assumed to follow a Poisson distribution with a mean of 35, which is the observed average number of pileup events at ATLAS during its data taking at the 13 TeV pp collisions.

III. RECONSTRUCTION AND IDENTIFICATION OF $H \to WW^*$ JETS

A. Event selection

Jets are reconstructed with the anti-k_T algorithm [42] with a distance parameter of $\Delta R = 1.0$, which is the default jet reconstruction algorithm used at the ATLAS and CMS experiments. To correct the presence of additional energy depositions from underlying events and pileups, we employ a jet area correction technique [43] to take into account the effects on an event-by-event basis. For each event, the distribution of transverse energy densities is calculated for all jets with $|\eta| < 2.1$, and its median is taken as an estimate of the energy density of the pileup and underlying events. We subsequently correct each jet by subtracting the product of the transverse energy density and the jet area, which is determined with the "active" area calculation technique [43]. This method results in a modified jet four-momentum $p^\mu = (m_{\text{jet}}, \vec{p}_{\text{jet}})$ that is used throughout the paper unless explicitly stated otherwise.

We select jets with $p_T > 350$ GeV and $|\eta| < 2.0$ as $H \to WW^*$ jet candidates. MC studies show that the averaged momentum of the $W^{(*)}$ bosons decayed from the Higgs boson is about 25 GeV in the Higgs rest frame, much smaller than the momenta of the selected $H \to WW^*$ jet candidates. As a result, the decaying products of the two $W^{(*)}$ bosons often overlap with each other. Figure 1 shows the efficiency to reconstruct a hadronically decaying $H \to WW^*$ using a single jet as a function of the Higgs boson p_T. The efficiency is defined as $\epsilon = N_{\text{reco}}/N_{\text{gen}}$, where N_{gen} is the number of generated Higgs bosons and N_{reco} is the number of reconstructed $H \to WW^*$ jet candidates whose separations between partons decayed from $W^{(*)}$ bosons and $H \to WW^*$ jet are less than 1. Here the separation between two objects is defined as $\Delta R = \sqrt{\Delta\eta^2 + \Delta\phi^2}$, where $\Delta\eta$ and $\Delta\phi$ are the differences in pseudorapidity and the azimuthal angle between the two objects' momenta, respectively. For a Higgs boson with $p_T = 350$ GeV, the averaged separation between the decaying products of $H \to WW^*$ is about 0.8, and approximately 55% of the $H \to WW^*$ in the hadronic final state can be reconstructed as a single jet. The averaged separation gradually decreases as a function of p_T to be less than

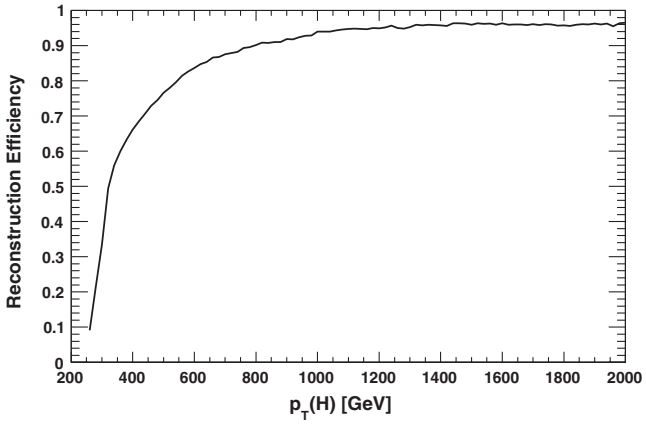

FIG. 1. The reconstruction efficiency of a hadronically decaying $H \to WW^*$ using a single jet as a function of the Higgs boson p_T. The Higgs bosons are required to have $|\eta| < 2.0$.

0.5 for Higgs bosons with $p_T > 1$ TeV, where more than 90% of the $H \to WW^*$ in the hadronic final state can be reconstructed as a single jet.

We further require the track-assisted mass [44] of selected $H \to WW^*$ jets to satisfy $40 < m_{\text{jet}}^{\text{TA}} < 240$ GeV. The track-assisted jet mass is defined as $m_{\text{jet}}^{\text{TA}} = m_{\text{jet}}^{\text{trk}} \times (p_T/p_{T,\text{jet}}^{\text{trk}})$, where $m_{\text{jet}}^{\text{trk}}$ and $p_T/p_{T,\text{jet}}^{\text{trk}}$ are the invariant mass and the total transverse momentum of charged tracks associated with the jet, respectively. Only charged tracks with $p_{\text{T}} > 1$ GeV and $|\eta| < 2.5$ are considered. They are also required to satisfy the criteria that $|d_0| < 1$ mm and $|z_0 - z_{\text{pv}}| \sin\theta < 1.5$ mm, where d_0 and z_0 are the transverse and longitudinal impact parameters of the charged track, respectively, z_{pv} is the longitudinal position of the primary vertex, and θ is the polar angle of the charged track. A charged track is considered to be associated with a jet with p_T in a unit of GeV only if the separation ΔR between the track and jet is less than R_{max}, where $R_{\text{max}} = 1.0 - 0.4 \times (p_T - 350)/650$ for jets with

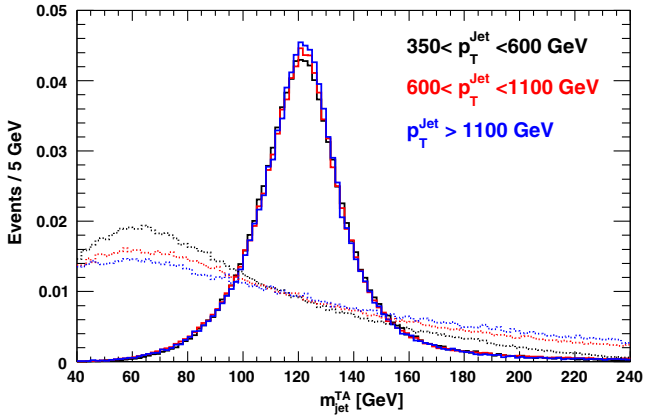

FIG. 2. The track-assisted jet mass distribution of signal $H \to WW^*$ jets (solid line) and QCD jets (dashed line) in different p_T ranges.

$p_T < 1000$ GeV and $R_{\max} = 0.6$ for jets with $p_T > 1000$ GeV, respectively. The track-assisted jet mass distributions of signal $H \to WW^*$ jets and QCD jets in different p_T ranges are shown in Fig. 2. The $m_{\text{jet}}^{\text{TA}}$ distribution of the signal jets peaks around the Higgs boson mass and its shape shows no significant variation as a function of jet p_T.

B. Jet substructure

Signal $H \to WW^*$ jets can be further distinguished from QCD jets using jet substructure variables. There are many jet substructure variables [45] proposed, and some of them have been successfully used to identify the boosted hadronically decaying W/Z boson, top quark, and $H \to b\bar{b}$ boson by the ATLAS [46,47] and CMS [48,49] experiments. As a simple illustration, this paper uses the substructure variables defined in the center-of-mass frame of the jet, introduced in Ref. [50]. They are the thrust (T), thrust minor (T_{min}), sphericity (S), and the ratio between the second-order and zeroth-order Fox-Wolfram moments (R_2). Those variables have been successfully implemented by the ATLAS experiment to make the first observation of the boosted hadronically decaying vector boson reconstructed as a single jet from the SM $W/Z +$ jets production [51].

We define the center-of-mass frame (rest frame) of a jet as the frame where the four-momentum of the jet is equal to $p_\mu^{\text{rest}} \equiv (m_{\text{jet}}, 0, 0, 0)$. All the jet substructure variables are calculated using the energy clusters of a jet or the charged tracks associated with a jet in the center-of-mass frame of the jet. Their distributions are shown in Fig. 3. A jet consists of its constituent particles. While the $H \to WW^*$ is a two-body decay, the momenta of the $W^{(*)}$ bosons in the Higgs rest frame are very small due to the mass suppression. As a result, the distribution of the constituent particles of a boosted $H \to WW^*$ in its center-of-mass frame has a four-body decay topology, with each subjet corresponding to one quark decayed from the two $W^{(*)}$ bosons. The hadronically decaying products from a boosted $H \to WW^*$ has a relatively isotropic distribution in the jet rest frame. It is worth noting that the tracks associated with a Higgs boson with a larger p_T are more isotropically distributed compared to the ones associated with a Higgs boson with a smaller p_T, as shown in Fig. 3. Such an effect is also seen in the distribution of jet sphericity calculated using the energy clusters but not for thrust, thrust minor, and R_2, as their calculations based on the energy clusters are degraded by the finite resolution of the Calorimeter detector when jet p_T becomes very large. On the other hand, the constituent particle distribution of a QCD jet in the jet rest frame is less isotropic and becomes even more directional when jet p_T becomes larger. As a result, the jet substructure variables defined in the jet rest frame has a better discriminating power to separate boosted $H \to WW^*$ bosons from the background for jets with larger p_T.

We further recluster the energy clusters of a jet to reconstruct subjets in the jet rest frame using a generalized EEkT algorithm [52] in the FASTJET3.0.1 [40] package with the parameters of $p = 0$ and $R = 0.8$. The reconstructed

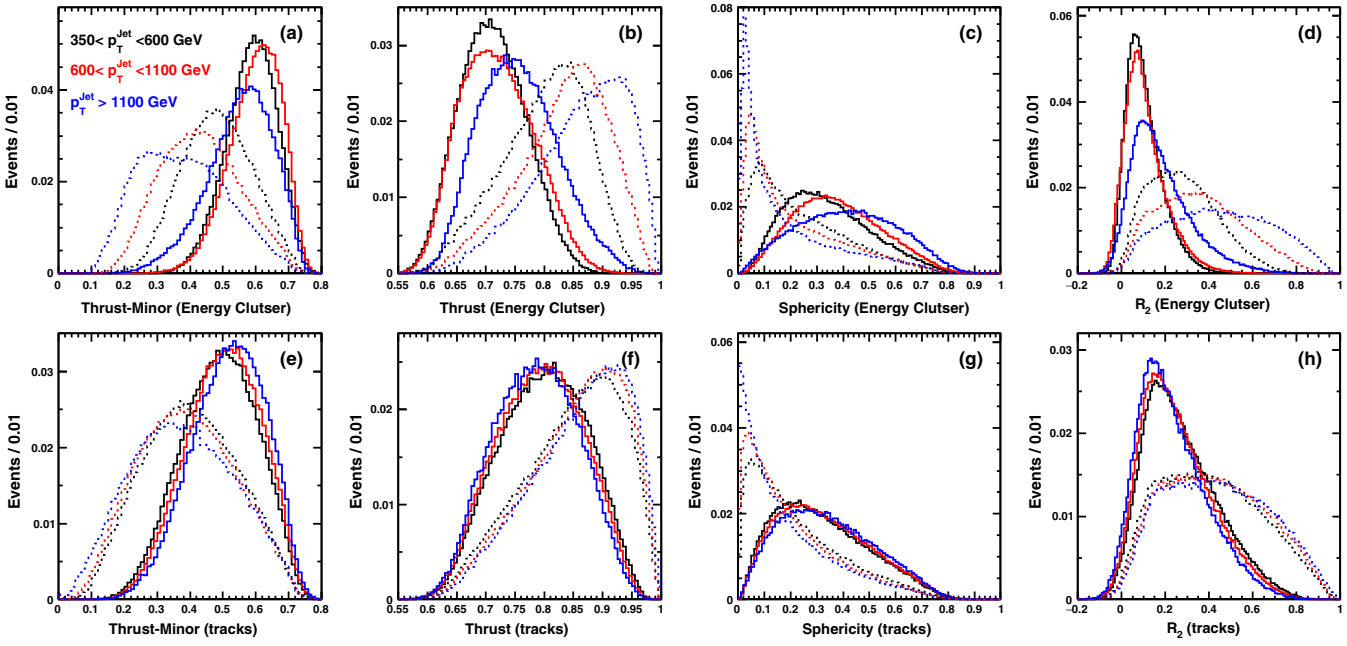

FIG. 3. The distributions of the jet substructure variables calculated using energy clusters (top row) of a jet or charged tracks (bottom row) associated with the jet for $H \to WW^*$ signal jets (solid line) and QCD jet background (dashed line) in different jet p_T ranges. Highly directional distributions of energy clusters or charged tracks have $T \approx 1$, $T_{\text{min}} \approx 0$, $S \approx 0$, and a large value of R_2, while $T \approx 0.5$, $T_{\text{min}} \approx 1$, $S \approx 1$, and a small value of R_2 correspond to an isotropic distribution. All the distributions are normalized to unity.

subjets are required to have energy $E_{\text{subjet}} > 10$ GeV in the jet rest frame. A charged track is considered to be associated with a subjet only if their angular separation is less than 0.8 in the jet rest frame.

C. Identification of $H \to WW^*$ jets

The final variable to identify boosted $H \to WW^*$ jets is constructed using a boosted decision tree (BDT) algorithm. The input variables used in the BDT include $m_{\text{jet}}^{\text{TA}}$, the number of charged tracks associated with the jet, the number of subjets reconstructed in the jet rest frame, and jet substructure variables (T, T_{min}, S, and R_2) calculated using energy clusters and charged tracks, respectively. Among all the input variables in the BDT, the best one to distinguish signal from background is $m_{\text{jet}}^{\text{TA}}$, which also does not have a strong correlation with the other variables. All the substructure variables have comparable discriminating powers, but they are highly correlated. The linear correlation efficiencies between them vary approximately between 60% and 90%. The number of subjet has slightly less discriminating power than jet substructure variables, and their correlations range between 20% and 50%. While the number of charged tracks has the least power to disentangle signal from background, its correlations to other variables are less than 10%. The signal identification efficiency of $H \to WW^*$ jets vs the background rejection of QCD jets for the BDT variable is shown in Fig. 4, where the signal identification efficiency is defined as the probability for a reconstructed signal $H \to WW^*$ jet to pass a given requirement of the BDT variable. The rejection of QCD jets for a given $H \to WW^*$ jet identification efficiency is comparable to the $H \to b\bar{b}$ taggers at ATLAS [53] and CMS [49]. The performance of $H \to WW^*$ identification gets better for jets with larger p_T unlike the $H \to b\bar{b}$ taggers, whose background rejections degrade when the jet p_T increases [49,53]. The performance of $H \to WW^*$ identification can be further improved by including additional BDT input variables, such as the subjet energies, the number of charged tracks associated with each subjet, other jet substructure variables [45] defined in the lab frame, and so on. Such a dedicated study is beyond the scope of this paper.

IV. APPLICATION

Reconstructed $H \to WW^*$ jets can be used to improve searches for NP with specific final state signatures. Here we demonstrate such an application by considering a search for a heavy resonance (X) with the narrow width that decays into two Higgs bosons in the final states: $pp \to X \to HH$, $H \to b\bar{b}, WW^*$, where both $W^{(*)}$ bosons decay hadronically. Note that for such high-mass (>1.5 TeV) resonance decays, more than 90% of the events have their decay particles from the Higgs decay within a cone of $R < 1.0$. As a result, two leading jets that have the highest and the second-highest energy with $p_T > 350$ GeV and $|\eta| < 2.0$ in an event are selected as two Higgs jet candidates. They are subsequently combined to form an $X \to HH$ resonance candidate. The $H \to b\bar{b}$ jet identification and the $H \to WW^*$ jet identification are subsequently applied to reduce the background that is dominated by QCD jets with the criteria that both identification efficiencies are set to be 50%. The background rejection of $H \to b\bar{b}$ tagger is assumed to be the same as the center-of-mass Higgs tagger [22,53] at ATLAS.

We estimate the expected 95% C.L. upper limit (UL) on the product of the production cross section of a heavy resonance X and the branching fraction for its decay into a Higgs boson pair. The expected limit is plotted as a function of the assumed X mass, as shown in Fig. 5, for 400 fb^{-1} LHC data at 13 TeV, equivalent to the total luminosity accumulated after the incoming run III data taken at the LHC. For heavy resonances whose masses are below

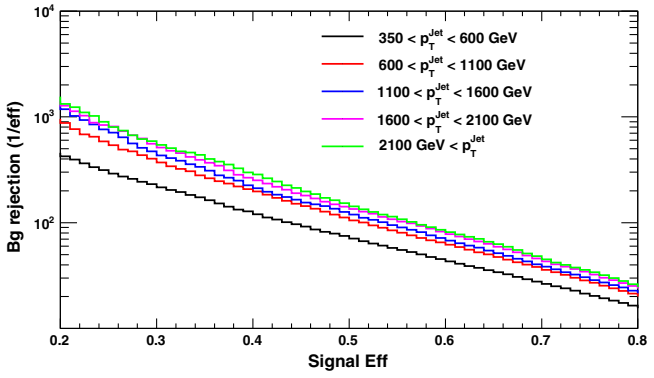

FIG. 4. The background rejection of QCD jets vs the signal efficiency of $H \to WW^*$ jets in different jet p_T ranges, where the background rejection is defined as $1/\epsilon_{\text{bg}}$ and ϵ_{bg} is the misidentification efficiency of the background QCD jets for a given signal identification efficiency.

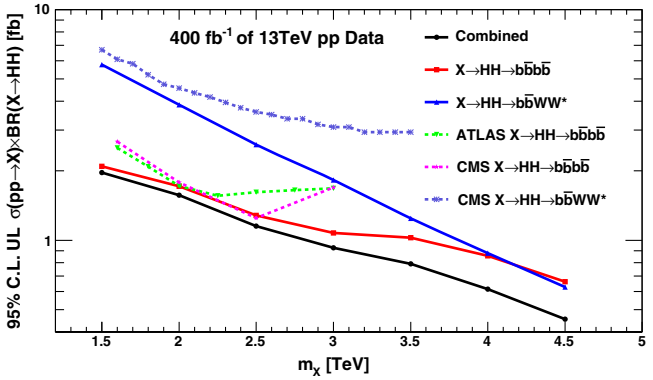

FIG. 5. The expected 95% C.L. UL on the product of the production cross section of a heavy resonance X and its decaying branching faction into a Higgs boson pair, as a function of the assumed X mass that is reconstructed in different Higgs boson decay final states.

3 TeV, the search sensitivity in the final state where both Higgs bosons decay into a $b\bar{b}$ pair ($X \to HH \to b\bar{b}b\bar{b}$) is significantly better than the final state in which one of the Higgs bosons decays into two $W^{(*)}$ bosons ($X \to HH \to b\bar{b}WW^*$) because of the much larger decay branching fraction of $H \to b\bar{b}$ than that of $H \to WW^*$ in the hadronic final state. However, the expected UL in the $X \to HH \to b\bar{b}WW^*$ final state becomes comparable to the one in the $X \to HH \to b\bar{b}b\bar{b}$ channel for resonances with masses above 3.5 TeV, due to the degradation of background rejection of $H \to b\bar{b}$ taggers for jets with very large p_T [22,53]. Besides $H \to b\bar{b}$ jets, adding $H \to WW^*$ jets as an additional experimental signature can lower the expected UL of searches for $X \to HH$ by 10%–50%, depending on the resonance mass.

We compare the search sensitivities in our study to the expected ones for 400 fb^{-1} data from the ATLAS and CMS experiments by scaling down their published results [17,20,34,36] according to the square root of the luminosity increase, as shown in Fig. 4. Our estimated UL in the $X \to HH \to b\bar{b}b\bar{b}$ final state is comparable to the ones from the ATLAS [17] and CMS [34] publications, for resonances with masses less than 2 TeV, but better in the higher mass region. This is because our study used a most recent $H \to b\bar{b}$ tagger at ATLAS [22,53] that has a significantly better performance than the Higgs taggers used in the previous ATLAS and CMS publications. Both the ATLAS [20] and CMS [36] experiments also carried out searches for $X \to HH \to b\bar{b}WW^*$ in the final state where one $W^{(*)}$ boson decays hadronically and the other $W^{(*)}$ boson decays leptonically. Depending on the resonance mass, the expected UL from the CMS (ATLAS) publication is approximately 1.2–2 (>10) times the expected UL in our study, where both hadronically decaying $W^{(*)}$ bosons are reconstructed as a single jet.

Note that the above comparisons do not have a strong dependence on the theoretical models used to generate heavy resonances as long as the resonances have much narrower widths than the detector resolution of the reconstructed $X \to HH$ candidates, which is typically a few hundred GeV and increases when the masses of the resonances become larger.

V. CONCLUSION

In this paper, we study the reconstruction and identification of $H \to WW^*$ with high transverse momentum, where both $W^{(*)}$ bosons decay hadronically. We show that the boosted $H \to WW^*$ can be effectively reconstructed as a single jet and identified using jet substructures in the center-of-mass frame of the jet. Such a reconstruction and identification approach can discriminate the boosted $H \to WW^*$ in the full hadronic final state from QCD jets. Our result will significantly improve experimental sensitivities of searches for potential NP beyond the SM in final states containing highly boosted Higgs bosons. The technique we proposed can be also directly applied to boosted $H \to ZZ^*$ in the full hadronic final state.

ACKNOWLEDGMENTS

This work is supported by the Office of Science of the U.S. Department of Energy under Contract No. DE-FG02-13ER42027.

[1] M. Schmaltz and D. Tucker-Smith, Little Higgs review, Annu. Rev. Nucl. Part. Sci. **55**, 229 (2005).
[2] K. Agashe, H. Davoudiasl, S. Gopalakrishna, T. Han, G. Y. Huang, G. Perez, Z. G. Si, and A. Soni, LHC signals for warped electroweak neutral gauge bosons, Phys. Rev. D **76**, 115015 (2007).
[3] K. Agashe, S. Gopalakrishna, T. Han, G. Y. Huang, and A. Soni, LHC signals for warped electroweak charged gauge bosons, Phys. Rev. D **80**, 075007 (2009).
[4] G. C. Branco, P. M. Ferreira, L. Lavoura, M. N. Rebelo, M. Sher, and J. P. Silva, Theory and phenomenology of two-Higgs-doublet models, Phys. Rep. **516**, 1 (2012).
[5] B. A. Dobrescu, P. J. Fox, and J. Kearney, Higgs-photon resonances, Eur. Phys. J. C **77**, 704 (2017).
[6] J. M. Butterworth, A. R. Davison, M. Rubin, and G. P. Salam, Jet Substructure as a New Higgs Search Channel at the LHC, Phys. Rev. Lett. **100**, 242001 (2008).
[7] A. Abdesselam, E. B. Kuutmann, U. Bitenc, G. Brooijmans, J. Butterworth, P. Bruckman de Renstrom, D. Buarque Franzosi, R. Buckingham, B. Chapleau, M. Dasgupta *et al.*, Boosted objects: A probe of beyond the Standard Model physics, Eur. Phys. J. C **71**, 1661 (2011).
[8] B. Di Micco, M. Gouzevitch, J. Mazzitelli, C. Vernieri, J. Alison, K. Androsov, J. Baglio, E. Bagnaschi, S. Banerjee, and P. Basler *et al.*, Higgs boson potential at colliders: Status and perspectives, Rev. Phys. **5**, 100045 (2020).
[9] ATLAS Collaboration, Search For Higgs Boson Pair Production in the $\gamma\gamma b\bar{b}$ Final State using pp Collision Data at $\sqrt{s} = 8$ TeV from the ATLAS Detector, Phys. Rev. Lett. **114**, 081802 (2015).
[10] ATLAS Collaboration, Search for a new resonance decaying to a W or Z boson and a Higgs boson in the $\ell\ell/\ell\nu/\nu\nu + b\bar{b}$ final states with the ATLAS detector, Eur. Phys. J. C **75**, 263 (2015).

[11] ATLAS Collaboration, Search for Higgs boson pair production in the $b\bar{b}b\bar{b}$ final state from pp collisions at $\sqrt{s} = 8$ TeVwith the ATLAS detector, Eur. Phys. J. C **75**, 412 (2015).
[12] ATLAS Collaboration, Searches for Higgs boson pair production in the $hh \to bb\tau\tau, \gamma\gamma WW^*, \gamma\gamma bb, bbbb$ channels with the ATLAS detector, Phys. Rev. D **92**, 092004 (2015).
[13] ATLAS Collaboration, Search for new resonances decaying to a W or Z boson and a Higgs boson in the $\ell^+\ell^- b\bar{b}$, $\ell\nu b\bar{b}$, and $\nu\bar{\nu}b\bar{b}$ channels with pp collisions at $\sqrt{s} = 13$ TeV with the ATLAS detector, Phys. Lett. B **765**, 32 (2017).
[14] ATLAS Collaboration, A search for resonances decaying into a Higgs boson and a new particle X in the $XH \to qqbb$ final state with the ATLAS detector, Phys. Lett. B **779**, 24 (2018).
[15] ATLAS Collaboration, Search for heavy resonances decaying to a W or Z boson and a Higgs boson in the $q\bar{q}^{(\prime)}b\bar{b}$ final state in pp collisions at $\sqrt{s} = 13$ TeV with the ATLAS detector, Phys. Lett. B **774**, 494 (2017).
[16] ATLAS Collaboration, Search for heavy resonances decaying into a W or Z boson and a Higgs boson in final states with leptons and b-jets in 36 fb^{-1} of $\sqrt{s} = 13$ TeV pp collisions with the ATLAS detector, J. High Energy Phys. 03 (2018) 174; Erratum, 11 (2018) 051.
[17] ATLAS Collaboration, Search for pair production of Higgs bosons in the $b\bar{b}b\bar{b}$ final state using proton-proton collisions at $\sqrt{s} = 13$ TeV with the ATLAS detector, J. High Energy Phys. 01 (2019) 030.
[18] ATLAS Collaboration, Combination of searches for heavy resonances decaying into bosonic and leptonic final states using 36 fb^{-1} of proton-proton collision data at $\sqrt{s} =$ 13 TeV with the ATLAS detector, Phys. Rev. D **98**, 052008 (2018).
[19] ATLAS Collaboration, Search for heavy resonances decaying to a photon and a hadronically decaying $Z/W/H$ boson in pp collisions at $\sqrt{s} = 13$ TeV with the ATLAS detector, Phys. Rev. D **98**, 032015 (2018).
[20] ATLAS Collaboration, Search for Higgs boson pair production in the $b\bar{b}WW^*$ decay mode at $\sqrt{s} = 13$ TeV with the ATLAS detector, J. High Energy Phys. 04 (2019) 092.
[21] ATLAS Collaboration, Search for resonances decaying into a weak vector boson and a Higgs boson in the fully hadronic final state produced in proton-proton collisions at $\sqrt{s} =$ 13 TeV with the ATLAS detector, Phys. Rev. D **102**, 112008 (2020).
[22] ATLAS Collaboration, Search for Heavy Resonances Decaying Into a Photon and a Hadronically Decaying Higgs Boson in pp Collisions at $\sqrt{s} = 13$ TeV with the ATLAS Detector, Phys. Rev. Lett. **125**, 251802 (2020).
[23] ATLAS Collaboration, Reconstruction and identification of boosted di-τ systems in a search for Higgs boson pairs using 13 TeV proton-proton collision data in ATLAS, J. High Energy Phys. 11 (2020) 163.
[24] CMS Collaboration, Search for narrow high-mass resonances in proton-proton collisions at $\sqrt{s} = 8$ TeV decaying to a Z and a Higgs boson, Phys. Lett. B **748**, 255 (2015).
[25] CMS Collaboration, Search for resonant pair production of Higgs bosons decaying to two bottom quark–antiquark pairs in proton–proton collisions at 8 TeV, Phys. Lett. B **749**, 560 (2015).
[26] CMS Collaboration, Search for a massive resonance decaying into a Higgs boson and a W or Z boson in hadronic final states in proton-proton collisions at $\sqrt{s} = 8$ TeV, J. High Energy Phys. 02 (2016) 145.
[27] CMS Collaboration, Search for massive WH resonances decaying into the $\ell\nu b\bar{b}$ final state at $\sqrt{s} = 8$ TeV, Eur. Phys. J. C **76**, 237 (2016).
[28] CMS Collaboration, Search for heavy resonances decaying to two Higgs bosons in final states containing four b quarks, Eur. Phys. J. C **76**, 371 (2016).
[29] CMS Collaboration, Search for heavy resonances decaying into a vector boson and a Higgs boson in final states with charged leptons, neutrinos, and b quarks, Phys. Lett. B **768**, 137 (2017).
[30] CMS Collaboration, Search for heavy resonances that decay into a vector boson and a Higgs boson in hadronic final states at $\sqrt{s} = 13$ TeV, Eur. Phys. J. C **77**, 636 (2017).
[31] CMS Collaboration, Search for a massive resonance decaying to a pair of Higgs bosons in the four b quark final state in proton-proton collisions at $\sqrt{s} = 13$ TeV, Phys. Lett. B **781**, 244 (2018).
[32] CMS Collaboration, Search for heavy resonances decaying into a vector boson and a Higgs boson in final states with charged leptons, neutrinos and b quarks at $\sqrt{s} = 13$ TeV, J. High Energy Phys. 11 (2018) 172.
[33] CMS Collaboration, Search for heavy resonances decaying into two Higgs bosons or into a Higgs boson and a W or Z boson in proton-proton collisions at 13 TeV, J. High Energy Phys. 01 (2019) 051.
[34] CMS Collaboration, Search for production of Higgs boson pairs in the four b quark final state using large-area jets in proton-proton collisions at $\sqrt{s} = 13$ TeV, J. High Energy Phys. 01 (2019) 040.
[35] CMS Collaboration, Search for Narrow $H\gamma$ Resonances in Proton-Proton Collisions at $\sqrt{s} = 13$ TeV, Phys. Rev. Lett. **122**, 081804 (2019).
[36] CMS Collaboration, Search for resonances decaying to a pair of Higgs bosons in the $b\bar{b}q\bar{q}'\ell\nu$ final state in proton-proton collisions at $\sqrt{s} = 13$ TeV, J. High Energy Phys. 10 (2019) 125.
[37] T. Sjöstrand, S. Mrenna, and P. Z. Skands, PYTHIA 6.4 Physics and Manual, J. High Energy Phys. 05 (2006) 026.
[38] T. Sjostrand, S. Mrenna, and P. Z. Skands, A brief introduction to PYTHIA 8.1, Comput. Phys. Commun. **178**, 852 (2008).
[39] ATLAS Collaboration, The ATLAS Experiment at the CERN large hadron collider, J. Instrum. **3**, S08003 (2008).
[40] M. Cacciari and G. P. Salam, Dispelling the N^3 myth for the k_t jet-finder, Phys. Lett. **641**, 57 (2006).
[41] ATLAS Collaboration, Expected performance of the ATLAS Experiment—Detector, trigger and physics, arXiv: 0901.0512.
[42] M. Cacciari, G. P. Salam, and G. Soyez, The anti-k_t jet clustering algorithm, J. High Energy Phys. 04 (2008) 063.
[43] M. Cacciari and G. P. Salam, Pileup subtraction using jet areas, Phys. Lett. B **659**, 119 (2008).
[44] ATLAS Collaboration, Jet mass reconstruction with the ATLAS detector in early run 2 data, Report No. ATLAS-CONF-2016-035.

[45] A. Altheimer, A. Arce, L. Asquith, J. Backus Mayes, E. Bergeaas Kuutmann, J. Berger, D. Bjergaard, L. Bryngemark, A. Buckley and J. Butterworth *et al.*, Boosted Objects and Jet Substructure at the LHC, Eur. Phys. J. C **74**, 2792 (2014).

[46] ATLAS Collaboration, Performance of top-quark and W-boson tagging with ATLAS in run 2 of the LHC, Eur. Phys. J. C **79**, 375 (2019).

[47] ATLAS Collaboration, Identification of boosted Higgs bosons decaying into b-quark pairs with the ATLAS detector at 13 TeV, Eur. Phys. J. C **79**, 836 (2019).

[48] CMS Collaboration, Identification techniques for highly boosted W bosons that decay into hadrons, J. High Energy Phys. 12 (2014) 017.

[49] CMS Collaboration, Identification of heavy-flavour jets with the CMS detector in pp collisions at 13 TeV, J. Instrum. **13**, P05011 (2018).

[50] C. Chen, New approach to identifying boosted hadronically-decaying particle using jet substructure in its center-of-mass frame, Phys. Rev. D **85**, 034007 (2012).

[51] ATLAS Collaboration, Measurement of the cross-section of high transverse momentum vector bosons reconstructed as single jets and studies of jet substructure in pp collisions at $\sqrt{s} = 7$ TeV with the ATLAS detector, New J. Phys. **16**, 113013 (2014).

[52] S. Catani, Y. L. Dokshitzer, M. Olsson, G. Turnock, and B. R. Webber, New clustering algorithm for multijet cross sections in e^+e^- annihilation, Phys. Lett. B **269**, 432 (1991).

[53] ATLAS Collaboration, Variable radius, exclusive-k$_T$, and center-of-mass subjet reconstruction for Higgs($\to b\bar{b}$) tagging in ATLAS, Report No. ATL-PHYS-PUB-2017-010.